^{13}C and ^{27}Al NMR Relaxation, Viscosity, and ^{1}H Diffusion Studies of an Ethylaluminum Dichloride Melt

Cynthia K. Larive,[†] Mengfin Lin,[†] Brian S. Kinnear,[‡] Bernard J. Piersma,[‡] Charles E. Keller,[§] and W. Robert Carper*,[⊥]

Department of Chemistry, University of Kansas, Lawrence, Kansas 66045; Department of Chemistry, Houghton College, Houghton, New York 14744; Department of Chemistry, P.O. Box 1901, Mississippi State University, Mississippi State, Mississippi 39762; and Department of Chemistry, Wichita State University, Wichita, Kansas 67260

Received: August 4, 1997; In Final Form: October 16, 1997

^{13}C and ^{27}Al NMR relaxation studies of a 1:1 1-ethyl-3-methylimidazolium chloride (MEICl)−ethylaluminum dichloride ($EtAlCl_2$) melt provide rotational correlation times for MEI^+ and $EtAlCl_2$ which are compared with viscosities and diffusion coefficients. Diffusion coefficients for MEICl and $EtAlCl_2$ in a 1:1 MEICl−$EtAlCl_2$ melt are determined simultaneously using ^{1}H diffusion ordered spectroscopy (DOSY). All MEI^+ diffusion coefficients (ring, methyl, and ethyl protons) are virtually identical at a given temperature as are the methylene and methyl protons of $EtAlCl_2$. The MEI^+ and $EtAlCl_2$ diffusion coefficients are viscosity dependent and correlate with ^{13}C and ^{27}Al NMR rotational correlation times, indicating that the transport properties of the 1:1 MEICl−$EtAlCl_2$ melt are determined by the molar quantities of salt and not by the properties of the individual ions. Microviscosity factors provide reasonable values for the radius of MEI^+ from both viscosity and ^{13}C NMR rotational correlation times. The "slip" model is used to describe the movement of MEI^+ in the 1:1 MEICl−$EtAlCl_2$ melt.

Introduction

Room-temperature chloroaluminate melts provide excellent model systems for NMR relaxation studies.[1−4] In addition to the room-temperature melts containing $AlCl_3$, similar molten salts using ethylaluminum dichloride ($EtAlCl_2$) instead of $AlCl_3$ have been reported and investigated by NMR.[5−7] The structure of ethylaluminum dichloride is that of a trans dimer with a mp of ≈32 °C.[8−11] The addition of solid MEICl to $EtAlCl_2$ produces a viscous melt whose mp is ≈−70 °C. The primary species in the 1:1 MEICl−$EtAlCl_2$ melt has been identified by ^{27}Al NMR as the $EtAlCl_2$ dimer which has an ^{27}Al NMR peak at 129 ppm relative to $Al(H_2O)_6^{3+}$.[6,7]

The combined use of NMR ^{1}H diffusion ordered spectroscopy (DOSY) and NMR relaxation methods provides useful information about the dynamics and structure of various chemical systems and chloroaluminate systems in particular.[3,4,12] This approach has been used to determine diffusion coefficients as a function of temperature for 1-ethyl-3-methylimidazolium chloride (MEICl) in 0.5, 0.8:1, and 1:1 $AlCl_3$−MEICl melts where the predominate cation and anions include MEI^+ (Figure 1) in all melts, $AlCl_4^-$ in the 0.8:1 and 1:1 melts, and $Al_2Cl_7^-$ in the 0.8:1 and 0.5:1 melts. The MEI^+ diffusion coefficients for these $AlCl_3$−MEICl melts are viscosity dependent and correlate with conductivities and ^{13}C correlation times.[3,4]

In this study we report ^{27}Al and ^{13}C relaxation rates and ^{1}H diffusion coefficients obtained from 22 to 62 °C for a 1:1 $EtAlCl_2$−MEICl melt. The ^{27}Al and ^{13}C NMR rotational correlation times obtained for $EtAlCl_2$ and MEI^+ in the 1:1 $AlCl_3$−MEICl melt are compared with viscosity and ^{1}H diffusion coefficients. In this study diffusion coefficients of more than one species are determined simultaneously and then used with NMR rotational correlation times and viscosity data to test various physical models as suggested by Boere and Kidd.[13]

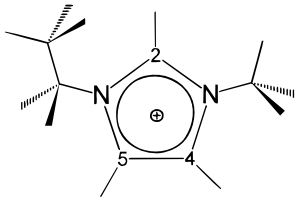

Figure 1. MEI cation (positions are labeled).

Experimental Section

Materials. The 1-ethyl-3-methylimidazolium chloride and chloroaluminate molten salts were prepared as previously described.[14] All materials were stored under anhydrous helium gas atmosphere in a drybox. All molten salt preparations and manipulations were performed in the drybox. Samples were loaded into 5 mm sample tubes, capped in the drybox, removed, and sealed immediately with a torch.

NMR Relaxation Measurements. ^{27}Al and ^{13}C NMR spectra were recorded on a Varian XL-300 spectrometer (78.15 and 75.43 MHz). Temperature measurements were calibrated against methanol or ethylene glycol and are accurate to within 0.5 °C. Pulse widths were typically 7−10 μs, and longitudinal relaxation times were measured by the inversion−recovery method (180°−τ−90°−T) with $T > 10T_1$. At least 12 delay times (τ) were used, and relaxation times (in duplicate) were

* To whom correspondence should be addressed. e-mail: Carper@wsuhub.uc.twsu.edu.
† University of Kansas.
‡ Houghton College.
§ Mississippi State University.
⊥ Witchita State University.

S1089-5647(97)02553-4 CCC: $15.00 © 1998 American Chemical Society
Published on Web 02/12/1998

obtained from a three-parameter exponential fit of magnetization as a function of τ. We failed to observe nonexponential behavior in any of the relaxation measurements. All R_1 values reported herein (estimated error <5% or less) are given in rad/s. Nuclear Overhauser effect (η') measurements were made using the gated decoupler method in which the fully decoupled spectrum is compared with one in which decoupling is present only during the acquisition time.[15] It is likely that the error in the nuclear Overhauser effect measurements is in the 5−10% range.[15]

Diffusion Coefficient Measurements. Diffusion coefficients were measured by pulsed field gradient ^{1}H NMR spectroscopy with the LED pulse sequence.[16] A slight modification of the standard LED sequence was employed in which the 90° read pulse was replaced by a 30° pulse to prevent overloading the receiver by the intense signals of the concentrated molten salt samples. The LED spectra were measured using a Bruker 500 MHz AM NMR spectrometer modified to accommodate pulsed field gradient experiments[17] and a 5 mm Bruker inverse probe with an actively shielded z gradient coil. The probe coil constant was calibrated using a D_2O solution of β-cyclodextrin and neat octanol and decanol at 25 °C which have self-diffusion coefficients similar to those of molten salts (3.2×10^{-6}, 1.4×10^{-6}, and 7.5×10^{-7} cm^2 s^{-1}, respectively).

Diffusion coefficients are obtained by collecting a series of ^{1}H NMR spectra measured as a function of gradient amplitude using the modified LED sequence. In the LED experiment, the resonance intensity depends on gradient area as follows:

$$I = I_0 \exp[-D(\Delta - \delta/3)\gamma^2 g^2 \delta^2] \quad (1)$$

where I_0 is the intensity of the resonance in the NMR spectrum in the absence of gradient pulses, γ is the magnetogyric ratio, Δ is the delay period during which molecular diffusion occurs, g and δ are the gradient amplitude and duration time, respectively, and D is the diffusion coefficient. In these experiments, the gradient duration time, δ, was 3 ms, the gradient amplitude was varied from 0.021 to 0.329 T m^{-1}, and the diffusion delay time selected as either 0.2 or 0.3 s.

Diffusion coefficients were calculated from the LED data using the DOSY methodology as described previously.[12,17−19] The individual free induction decays were transferred to a Silicon Graphics Indigo workstation and processed using Felix 2.30 (Biosym). Following Fourier transformation, phasing, and baseline correction, diffusion coefficients were extracted using the program SPLMOD.[20,21]

Viscosity Measurements. Kinematic viscosities were determined using calibrated Cannon-Fenske viscometers. The viscometers were filled and then placed in a constant temperature bath in a drybox. Density measurements were made in a similar manner in the same drybox. Viscosity and density measurements of neat $EtAlCl_2$ (mp ≈ 32 °C) were extremely difficult below 50 and above 70 °C. Consequently, viscosity and density measurements of neat $EtAlCl_2$ were confined to temperatures between 52 and 70 °C. Viscosity and density measurements of the 1:1 $EtAlCl_2$−MEICl melt were relatively simple by comparison and were measured between 24 and 75 °C.

Results

Viscosity. The viscosity of the 1:1 $EtAlCl_2$−MEICl melt was determined between 24 and 75 °C. For comparison, the viscosity of neat $EtAlCl_2$ (mp ≈ 32 °C) was determined between 52 and 70 °C. At 70 °C, the viscosity of 1:1 $EtAlCl_2$−MEICl is 6.337 cP and that of neat $EtAlCl_2$ is only 1.223 cP. The difference in viscosities between 1:1 $EtAlCl_2$−MEICl and dimeric $EtAlCl_2$ is consistent with molecular interactions between various species in the 1:1 $EtAlCl_2$−MEICl melt. A plot of ln viscosity vs reciprocal temperature for the 1:1 $EtAlCl_2$−MEICl melt and neat $EtAlCl_2$ (Figure 2) yields activation energies of 4.39 kcal for the 1:1 $EtAlCl_2$−MEICl melt and 3.06 kcal for the neat $EtAlCl_2$ with correlation coefficients of 0.999 for both sets of data.

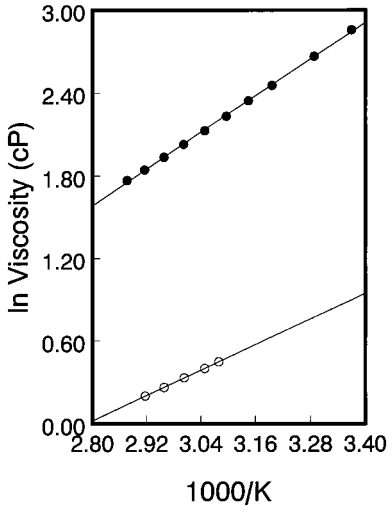

Figure 2. Plot of ln viscosity (cP) vs 1000/T for 1:1 $EtAlCl_2$−MEICl Melt (●) and neat $EtAlCl_2$ (○).

^{13}C Dipolar Relaxation. For the "extreme narrowing condition ($\omega\tau \ll 1$)", which characterizes the motion of small molecules or complexes, the dipolar relaxation for ^{13}C relaxed by ^{1}H is given by[22]

$$R_1^{dd} = N_H(h\gamma_C\gamma_H)^2 r_{CH}^{-6}\tau_c \quad (2)$$

where N_H is the number of hydrogens attached directly to the carbon atom, γ_C and γ_H are magnetogyric ratios, and r_{CH} = 1.09 Å. The effective correlation time, τ_c, varies with temperature and may be thought of as the time required for a nucleus to rotate through a distance of 1 rad.[22a] In actuality, the correlation time is the integral with respect to time from 0 to ∞ of the normalized autocorrelation function.[22b] The dipolar relaxation rate, R_1^{dd}, is calculated directly from the nuclear Overhauser enhancement factor, η', where $\eta'_{max} = \gamma_H/2\gamma_C$ = 1.988 for ^{13}C:[23]

$$R_1^{dd} = \eta' R_1/1.988 \quad (3)$$

^{27}Al Quadrupole Relaxation. In a manner similar to dipolar relaxation mechanisms, a nucleus of spin greater than $^1/_2$ that relaxes primarily through a quadrupolar mechanism also can be used as a NMR "probe" to monitor isotropic molecular tumbling. If there is a distortion from cubic symmetry, nuclei such as ^{27}Al will be under the influence of an electric field gradient which produces the quadrupole interaction. The quadrupole interaction is affected by the reorientation motion of the ^{27}Al-containing molecule ($EtAlCl_2$ in this case), and the quadrupolar relaxation rate in the "extreme narrowing region ($\omega\tau \ll 1$)" is given by[22,24]

$$R_1 = 1/T_1 = [3\pi^2(2I+3)/10I^2(2I-1)][1 + (\eta'^2/3)][e^2Qq/h]^2\tau_c \quad (4)$$

where $I = {}^5/_2$ for ^{27}Al, eQ is the nuclear electric quadrupole

TABLE 1: Average Correlation Times (ps) and Related Data for MEI^+ in a 1:1 MEICl−$EtAlCl_2$ Melt at 75.43 MHz

	η'		R_1(dipolar)		CT (ps)	
temp (°C)	C2	C4−5	C2	C4−5	C2	C4−5
25	1.90	1.98	0.489	0.569	22.9	26.7
27.5	1.90	1.98	0.464	0.543	21.7	25.4
30	1.88	1.96	0.446	0.505	20.9	23.6
32.5	1.84	1.92	0.418	0.456	19.6	21.3
35	1.84	1.91	0.382	0.434	17.9	20.3
37.5	1.82	1.91	0.353	0.396	16.5	18.5
40	1.80	1.89	0.319	0.373	14.9	17.5
42.5	1.79	1.87	0.293	0.350	13.7	16.4
45	1.77	1.84	0.278	0.320	13.0	15.0
47.5	1.76	1.80	0.259	0.289	12.1	13.5
50	1.76	1.81	0.253	0.278	11.9	13.0
52.5	1.74	1.79	0.239	0.263	11.2	12.3
55	1.71	1.78	0.223	0.256	10.4	12.0
57.5	1.69	1.75	0.203	0.240	9.5	11.2
60	1.65	1.74	0.193	0.221	9.0	10.3
62.5	1.65	1.72	0.188	0.213	8.8	10.0
65	1.63	1.72	0.174	0.201	8.2	9.4
67.5	1.63	1.69	0.158	0.187	7.4	8.7
70	1.60	1.67	0.150	0.179	7.0	8.4

moment, eq is the maximum component of the electric field gradient tensor, and η' is the asymmetry parameter of the electric field gradient tensor. τ_c is the effective correlation time and varies exponentially with temperature. The quadrupole coupling constant, χ, is given by

$$\chi = e^2Qq/h \tag{5}$$

NMR Correlation Times. In classical mechanics, the correlation time, τ_c, of a spherical particle undergoing isotropic rotation is[13]

$$\tau_c = 4\pi a^3\eta/3kT = V\eta/kT \tag{6}$$

Comparison of experimental data with correlation times calculated from eq 6 is generally unsuccessful as the theoretical correlation times are generally too large by a factor of 10, particularly in nonviscous fluids.[25−29]

For correlation times determined by NMR, the relationship between τ_c and temperature in the viscosity-dependent region is[13]

$$\tau_c = \tau_0 + (\eta\tau_{red}/T) \tag{7}$$

where $\tau_{red} = V/k$. The values of a, the hydrodynamic radius, obtained from this type of analysis are typically too small and are often corrected using a nonspherical rotational model. The other parameter obtained from this type of analysis is τ_0 which has been equated with free rotation times ($\tau_{fr} = [(2\pi/9)(I_m/kT)^{1/2}]$) by other investigators. However, this is a questionable interpretation as it represents an extrapolation out of the hydrodynamic region, through the kinetic region, and into the inertial limit of a completely free rotor model.[13]

MEI^+ ^{13}C Correlation Times. NMR ^{13}C correlation times for MEI^+ in the 1:1 $EtAlCl_2$−MEICl melt were calculated from eqs 2 and 3 using data from Table 1. Figure 3 contains a plot of ^{13}C NMR correlation times vs η/T for the 1:1 $EtAlCl_2$−MEICl melt between 25 and 70 °C. The ^{13}C NMR correlation times are the C2 and C4−5 (averaged) carbons of MEI^+ (Figure 1) and are assumed to be representative of the rotational motion of the MEI^+ molecular "framework". The value of τ_{red} (= V/k) obtained from the slopes in Figure 3 ($R_{val} = 0.999$) are 427.0 and 487.2 ps K cP^{-1} for MEI^+. These slopes produce calculated values of 1.12 and 1.17 Å or an average value of 1.15 Å for the radii of a spherical tumbling model of MEI^+ in the 1:1 MEICl−$EtAlCl_2$ melt. The MEI^+ average a value of 1.15 Å obtained for this melt is comparable to the value of 1.04 Å obtained for MEI^+ in a 1:1 MEICl−$AlCl_3$ melt although it is smaller than expected and will be reexamined later on in this report.[3,25−29]

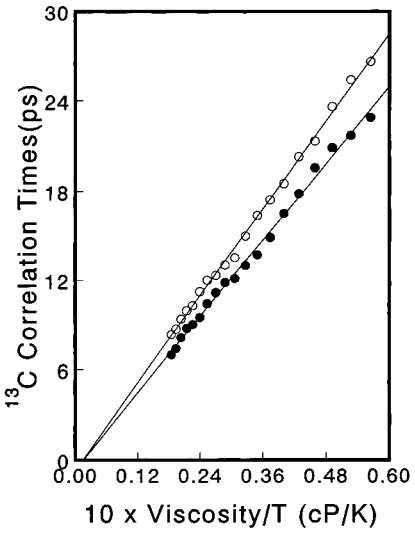

Figure 3. NMR ^{13}C correlation times (ps) for C2 (●) and C4−5 (○) vs viscosity/T (cP/K) for MEI^+ in a 1:1 $EtAlCl_2$−MEICl melt.

Diffusion Coefficients. The hydrodynamic basis for determining the rotational frictional coefficient for a sphere of radius a rotating in a medium of viscosity η was introduced by Stokes and then used by Einstein to describe Brownian motion of small particles. The resulting Stokes−Einstein equation based on viscous (frictional) drag gives the relationship between the diffusion coefficient and the radius (a) of a spherical particle moving (Brownian motion) in a continuous medium of macroscopic viscosity (η):

$$D = kT/6\pi\eta a \tag{8}$$

The use of eq 8 assumes that the molecular diameter does not change, and the original derivation is valid only for dilute solutions and not for highly concentrated molten salts.[29] Furthermore, the derivation leading to eq 8 applies only to spherical molecules moving in a continuum.[29] An alternate form of eq 8 is that proposed by McLaughlin in which the 6 in eq 8 is replaced by a 4.[30] This correction[30] is based on the introduction of a coefficient of sliding friction between the particle (solute) and the medium (solvent) and assumes that both solute and solvent are of similar radius.

Diffusion coefficients of MEI^+ were determined for the 1:1 $EtAlCl_2$−MEICl melt between 22 and 62 °C. Figure 4 is the DOSY spectrum of the 1:1 $EtAlCl_2$−MEICl melt at 40 °C. DOSY spectra are contour maps with NMR chemical shift and negative log diffusion coefficient along the two axes. There is a third dimension, intensity, which is shown in the projections along the NMR and diffusion dimensions. As expected, the diffusion coefficients from each MEI^+ ^1H resonance and each $EtAlCl_2$ ^1H resonance are equivalent within the experimental error of the measurement. The diffusion coefficients at 40 °C are $(1.08 \pm 0.01) \times 10^{-6}$ cm^2 s^{-1} for MEI^+ and $(1.54 \pm 0.04) \times 10^{-6}$ cm^2 s^{-1} for $EtAlCl_2$. The diffusion coefficient for neat $EtAlCl_2$ at 40 °C is $(12.2 \pm 0.14) \times 10^{-6}$ cm^2 s^{-1}, or approximately 8 times the value obtained for $EtAlCl_2$ in the 1:1 MEICl−$EtAlCl_2$ melt at 40 °C.

A plot of ln D vs reciprocal temperature for both the MEI^+ and $EtAlCl_2$ species is shown in Figure 5. For comparison, a

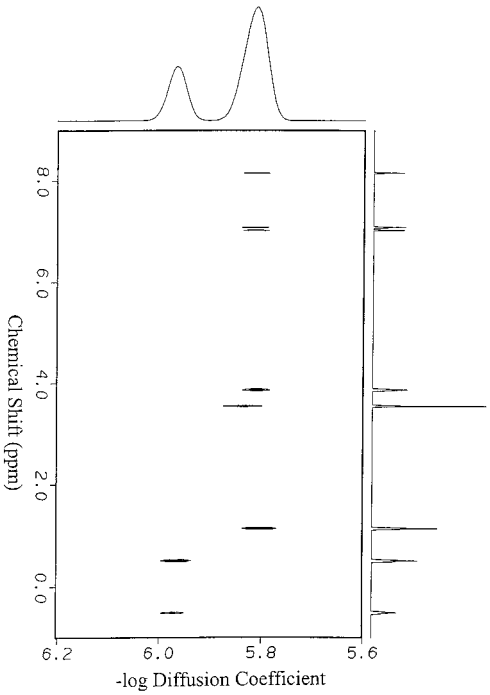

Figure 4. DOSY spectrum of $EtAlCl_2$−MEICl melt, 1:1 ratio, at 40 °C. The contours in this spectrum correlate ^1H chemical shift with the negative log of the diffusion coefficient. The projection plotted at the right of the contour map corresponds to the one-dimensional ^1H NMR spectrum. The spectrum was calculated from 21 individual LED spectra, each composed of 2048 real data points. The number of points in the diffusion dimension of the calculated spectrum was 512.

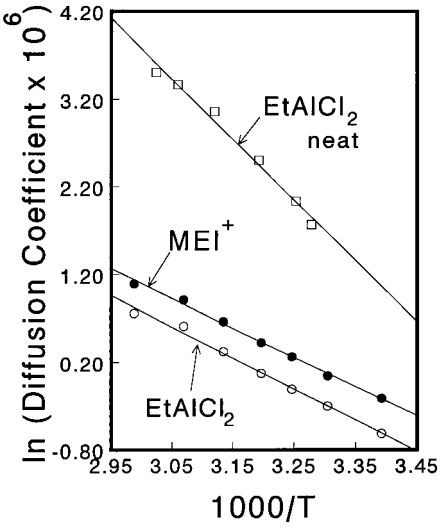

Figure 5. Plot of 1/diffusion coefficient (s/cm^2) vs reciprocal temperature for MEI^+ (●) and $EtAlCl_2$ (○) in a 1:1 $EtAlCl_2$−MEICl melt and neat $EtAlCl_2$ (□).

plot of the ln D data for neat $EtAlCl_2$ is included. The activation energies are 6.7 and 7.1 kcal for MEI^+ (R_{val} = 0.998) and $EtAlCl_2$ (R_{val} = 0.996) for the 1:1 MEICl−$EtAlCl_2$ melt between 22 and 62 °C. The activation energy of the neat (dimeric) $EtAlCl_2$ is 13.7 kcal (R_{val} = 0.998) between 32 and 58 °C, or approximately twice the activation energy found for $EtAlCl_2$ in the 1:1 MEICl−$EtAlCl_2$ melt.

Diffusion and Viscosities. A plot of 1/D vs η/T for the 1:1 MEICl−$EtAlCl_2$ melt and neat $EtAlCl_2$ (both the 1/D and η/T values for neat $EtAlCl_2$ have been increased by a factor of 10 for visualization purposes) is shown in Figure 6. The plots appear to have two distinct regions (or phases) which occur in

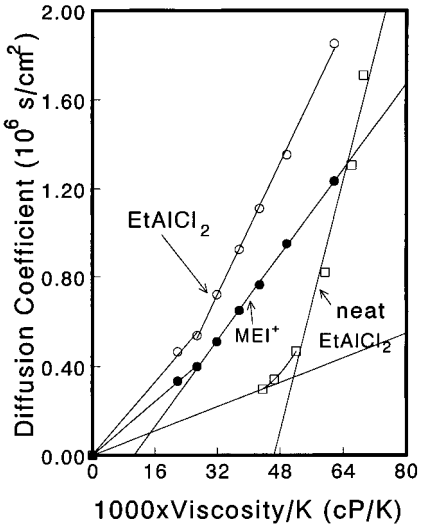

Figure 6. Plot of 1/diffusion coefficient (s/cm^2) vs viscosity/T (cP/K) for MEI^+ (●) and $EtAlCl_2$ (○) in a 1:1 $EtAlCl_2$−MEICl melt and neat $EtAlCl_2$ (□).

the vicinity of 55 °C. This is the same temperature where the ^{13}C NMR spin−spin (transverse) relaxation rates of neat $EtAlCl_2$ undergo changes similar to those observed for phase changes in other melts.[31] The linear plots (below 55 °C) in Figure 6 have slopes of 24.13 × 10^6, 37.36 × 10^6, and 70.70 × 10^6 s K/(cm^2 cP) (R_{val} = 0.999, 0.999, and 0.982) for MEI^+, $EtAlCl_2$ in the 1:1 melt, and neat $EtAlCl_2$. Analysis of these data using eq 8 produces hydrodynamic radii of 1.77 Å for MEI^+, 2.74 Å for $EtAlCl_2$ in the melt, and 5.19 Å for neat $EtAlCl_2$. The value of 1.77 Å for MEI^+ may be compared with values of 1.16 and 1.33 Å reported for MEI^+ in 1:1 and 2:1 $AlCl_3$−MEICl melts where the corresponding anions are $AlCl_4^-$ and $Al_2Cl_7^-$.[3,4] These slopes yield hydrodynamic a values of 2.66, 4.11, and 7.79 Å for MEI^+, $EtAlCl_2$ in the melt, and neat $EtAlCl_2$ using McLaughlin's modification of eq 8.[30] The 1:1 $EtAlCl_2$−MEICl melt produces a Stokes radius for MEI^+ that is smaller than the 3.2 Å value indicated previously on the basis of MOPAC calculations of MEI^+.[3,32]

Microdynamical Analysis by NMR. It is possible to relate the diffusion coefficient directly to the rotational correlation time by eliminating the viscosity term in eqs 7 and 8:

$$\tau_c = a^2/4.5D + \tau_0 \qquad (9)$$

A possible modification of eq 9 involves the use of the McLaughlin correction factor,[30] which replaces the 4.5 in eq 7 by 3. Equation 9 provides the direct relationship between measurements that can both be made by NMR under certain conditions as discussed below. Unfortunately, although eq 9 may prove useful, it does not solve any fundamental weaknesses that may exist in the derivations of eqs 6 and 8.

^{13}C NMR Rotational Correlation Times of MEI^+. The results are shown in Figure 7, in which the MEI^+ ^{13}C NMR correlation times for C2 and C4−C5 (averaged) from Table 1 are plotted vs 1/D. The slopes are 17.7 × 10^{-18} and 20.5 × 10^{-18} cm^2 for C2 and C4−C5 with τ_0's of 3.7 and 3.9 ps. The slopes are used to calculate values of 0.89 and 0.96 Å for an average hydrodynamic radius of 0.93 Å for MEI^+ a using eq 9 and 0.76 Å using McLaughlin's modification.[30] These values compare favorably with MEI^+ hydrodynamic radii of 0.95 and 0.77 Å (corrected) reported for a 1:1 $AlCl_3$−MEICl melt.[3] Despite this limited success, it is apparent that any sources of error (derivation of eq 8) in the classical model that relates

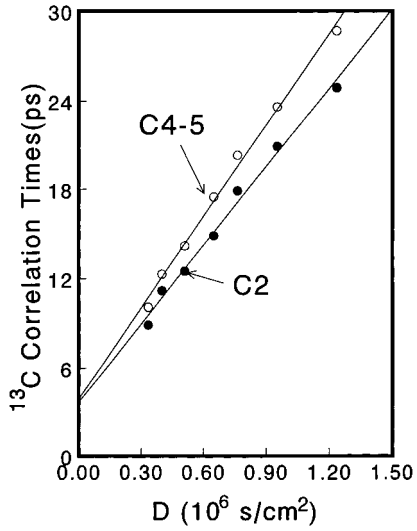

Figure 7. MEI$^+$ ^{13}C C2 (●) and (C4 + C5)/2 (○) correlation times (ps) vs $1/10^6$ × diffusion coefficients (s/cm^2) for a 1:1 $EtAlCl_2$−MEICl melt from 26 to 57 °C.

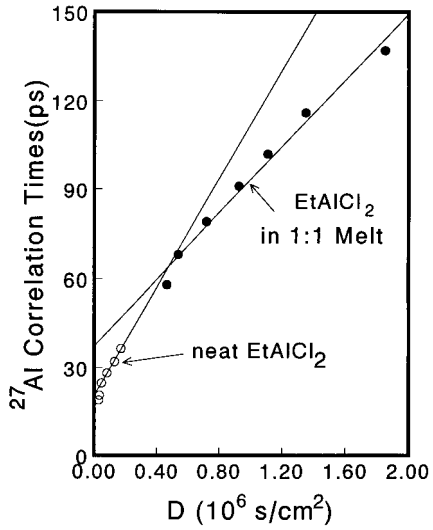

Figure 8. $EtAlCl_2$ ^{27}Al correlation times (ps) in a 1:1 $EtAlCl_2$−MEICl melt (●) and neat $EtAlCl_2$ (○) vs $1/10^6$ × diffusion coefficients (s/cm^2) for a 1:1 $EtAlCl_2$−MEICl melt and neat $EtAlCl_2$.

viscosity to correlation times (eq 6) produce a smaller hydrodynamic radius rather than a larger hydrodynamic radius.

^{27}Al NMR Rotational Correlation Times of $EtAlCl_2$. The results are shown in Figure 8, in which ^{27}Al NMR correlation times for $EtAlCl_2$ in the 1:1 MEICl−$EtAlCl_2$ melt are plotted vs $1/D$. The correlation times are calculated from eq 4 using ^{27}Al relaxation rates obtained at 129 ppm relative to $Al(H_2O)_6^{3+}$ and $[1 + (\eta'^2/3)]^{1/2}[\chi]$ values of 9.39 MHz for $EtAlCl_2$ in the 1:1 melt[33] and 25.50 MHz for neat $EtAlCl_2$.[34] It is assumed that the values for $[1 + (\eta'^2/3)]^{1/2}[\chi]$ do not undergo any significant changes over the temperature range of this study (approximately 25−65 °C).

Consistent with the change in relaxation properties of $EtAlCl_2$ above 55 °C, the ^{27}Al rotational correlation time data below 55 °C is analyzed with eq 9. The slopes are 56.1×10^{-18} and 91.5×10^{-18} cm^2 for $EtAlCl_2$ in the 1:1 melt and neat $EtAlCl_2$. The slopes are used with eq 9 to calculate a values of 1.59 and 2.03 Å for $EtAlCl_2$ in the 1:1 melt and neat $EtAlCl_2$, respectively. Values of 1.30 and 1.66 Å are obtained for $EtAlCl_2$ in the 1:1 melt and neat $EtAlCl_2$ using McLaughlin's modification.[30] Values for τ_0 are 37.3 ps for $EtAlCl_2$ in the 1:1 melt and 20.5 ps for neat $EtAlCl_2$, compared with a τ_0 value of 3.8 ps for MEI$^+$ (Figure 7). The τ_0 values for $EtAlCl_2$ correlate with the viscosities of these systems. The τ_0 values also indicate that the $EtAlCl_2$ species both in the 1:1 $EtAlCl_2$−MEICl melt and in neat $EtAlCl_2$ are larger than MEI$^+$.

Hydrodynamic Radii of MEI$^+$ and $EtAlCl_2$. Despite the correlations shown in this and previous reports, the values obtained for the hydrodynamic radii of MEI$^+$ and $EtAlCl_2$ are obviously less than any value obtained by theoretical methods. Other investigators have indicated that eq 6 is valid for large particles in a continuous medium but not for diffusing particles. In addition, there is the questionable relationship between a translational property (viscosity) and a rotational motion (rotational correlation time).[27−29] However, the results in Figures 3 and 6−8 indicate that there is a relationship between diffusion coefficients, correlation times, and viscosity that may be justifiable on a theoretical basis.

Comparison of Correlation Times, Diffusion Coefficients, and Viscosities. At 30 °C, the viscosity of the 1:1 $EtAlCl_2$−MEICl melt (14.76 cP) is similar to that of the 2:1 $AlCl_3$−MEICl acidic melt (15.47 cP) and higher than that of the 1:1 $AlCl_3$−MEICl melt (11.83 cP).[35] This is the opposite of what would be expected based on the fact that $AlCl_4^-$ (1:1 melt) is closer to MEI$^+$ in size than is either $Al_2Cl_7^-$ (2:1 $AlCl_3$−MEICl melt) or dimeric $EtAlCl_2$. At the same time, the MEI$^+$ diffusion coefficient is higher in both the 2:1 and 1:1 $AlCl_3$−MEICl melts than in the 1:1 $EtAlCl_2$−MEICl melt (1.44×10^{-6} and 1.27×10^{-6} cm^2 s^{-1} vs 1.05×10^{-6} cm^2 s^{-1}), and the MEI$^+$ ^{13}C rotational correlation time is longer in both the 1:1 $AlCl_3$−MEICl melt (23 ps) and the 1:1 $EtAlCl_2$−MEICl melt (22.5 ps) than in the 2:1 $EtAlCl_2$−MEICl melt (ps).[3,4] The evidence clearly points to a slower MEI$^+$ rotational motion in the 1:1 $AlCl_3$−MEICl and 1:1 $EtAlCl_2$−MEICl melts than in the 2:1 $AlCl_3$−MEICl melt. This supports the existence of MEI$^+$−$EtAlCl_2$ interactions in the 1:1 $EtAlCl_2$−MEICl melt. It is assumed that such interactions between MEI$^+$ and a form of dimeric $EtAlCl_2$ are similar to those reported for MEI$^+$ and $AlCl_4^-$ in the 1:1 $AlCl_3$−MEICl complex.[2,36−39]

Comparison of Classical and Nonspherical Rotational Models. The only obvious difference between the 1:1 $EtAlCl_3$−MEICl and 1:1 $AlCl_3$−MEICl melts appears to be the size and shape of the species that interact with MEI$^+$. The values of the MEI$^+$ hydrodynamic radius are seen to be similar in both melts, albeit smaller than a radius of approximately 3.2 Å obtained from crystallographic measurements[40] and gas-phase calculations.[4] In the case of the 1:1 $AlCl_3$−MEICl melt, the classical model of a sphere rotating in a continuous medium was adjusted to rationalize low a values obtained either directly or indirectly from eqs 6−9.[3] The "slip" boundary condition was assumed in which the spherical rotating molecule (MEI$^+$) has a radius approaching that of the solvent molecule and slips through the solvent provided that rotation can occur without solvent displacement. MEI$^+$ is not spherical in shape (Figure 1) and is closer to a prolate ($a = b < c$) spheroid whose rotation is anisotropic. This resulted in an approximate radius of MEI$^+$ (≈3.2 Å) that is considerably smaller than its maximum radius of 4.6 Å. The value of 3.2 Å is similar to the radius of $AlCl_4^-$ in the 1:1 $AlCl_3$−MEICl melt.

Molecular Sizes of MEI$^+$ and $EtAlCl_2$. Unfortunately, the molecular "size" relationship between MEI$^+$ and the trans dimer of $EtAlCl_2$ is difficult to estimate. The trans dimer of $EtAlCl_2$ is larger than MEI$^+$ in at least one dimension and can be classified as a prolate spheroid whereas MEI$^+$ may be considered as an oblate spheroid. Figure 9 contains the theoretical

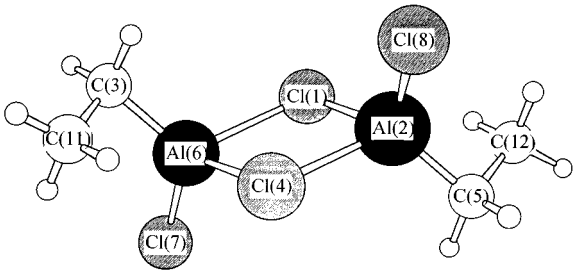

Figure 9. MOPAC(PM3)-optimized structure of the *trans*-$EtAlCl_2$ dimer.

structure of the trans dimer of $EtAlCl_2$ calculated using PM3.[40] The bond lengths (angtroms) in the trans $EtAlCl_2$ dimer (Figure 9) are as follows: Al(2)−Cl(1) = Al(6)−Cl(4) = 2.394, Al(2)−Cl(4) = 2.399, Al(6)−Cl(1) = 2.398, Al(6)−C(3) = Al(2)−C(5) = 1.874, Al(6)−Cl(7) = Al(2)−Cl(8) = 2.000, C(3)−C(11) = 1.500, C(5)−C(12) = 1.501. The bond angles (degrees) in the four-membered ring are as follows: Al(2)−Cl(1)−Al(6) = 104.73, Al(2)−Cl(4)−Al(6) = 104.72, Cl(1)−Al(2)−Cl(4) = 75.29, Cl(1)−Al(6)−Cl(4) = 75.28.

Unlike $AlCl_4^-$ which approximates a spherical model similar in size to MEI^+, the trans dimer of $EtAlCl_2$ is ellipsoidal in shape and larger than $AlCl_4^-$ (Figure 9). In $AlCl_4^-$, the average Al−Cl bond length is 2.169 Å, resulting in an ionic radius of 3.2 Å.[4] Unlike the spherical $AlCl_4^-$, the trans $EtAlCl_2$ dimer (Figure 9) occupies an ellipsoidal region whose dimensions are aproximately 4 × 4 × 9 Å.

Gierer−Wirtz Model. The classical "stick" or Stokes−Einstein frictional model does not appear to represent the 1:1 $EtAlCl_2$−MEICl melt in eq 6. Typically, one has to adjust the classical model of a sphere rotating in a continuous medium to account for the results obtained from eq 6. In view of the fact that solute−solvent interactions may be weak in the 1:1 melts and that the radius of MEI^+ is considerably smaller than dimeric $EtAlCl_2$, it is possible that the Gierer−Wirtz "slip" boundary condition[41] is met in 1:1 $EtAlCl_2$−MEICl melt as it is in the 1:1 $AlCl_3$−MEICl melt. In the "slip" boundary condition the spherical rotating molecule has a radius approaching that of the solvent molecule and slips through the solvent provided that rotation can occur without solvent displacement.[41] This microviscosity factor is to be used with the Stokes−Einstein−Debye equation (eq 6) to produce realistic values of correlation times.[13] The Gierer−Wirtz microviscosity factor can only be calculated from a spherical model that requires an approximate or average ionic radii for MEI^+ and *trans*-$EtAlCl_2$. This results in average effective ionic radii of 3.2 and 5.2 Å for MEI^+ and the *trans*-$EtAlCl_2$ dimer, obtained from molecular volumes. Using these ionic radii, one obtains a "slip" microviscosity correction factor of 0.254 similar to that used for MEI^+ and $Al_2Cl_7^-$ in the 2:1 $AlCl_3$−MEICl melt.[4] This would effectively increase the *a* values obtained using eq 7 from 1.12 and 1.17 Å to 1.77 and 1.85 Å. This correction[41] is typical;[13] however, it assumes a spherical particle and not either a prolate or oblate spheroid, both of which are present in the 1:1 $EtAlCl_2$−MEICl melt. In addition, both models must be considered for MEI^+ as it may undergo rotational motion either about the axis that passes parallel to the extended methyl and ethyl groups or about an axis perpendicular to the imidazole ring. In a similar manner, the trans dimer may undergo rotation about either its major or its minor axes.

Hu−Zwanzig Model. The Hu−Zwanzig model[42] allows for the existence of oblate and prolate spheroids, and both "slip" and "stick" factors have been calculated for these shapes. The ratio of the minimum:maximum axis of MEI^+ is ≈0.60, which produces an oblate slip microviscosity factor of 0.096 and a prolate slip microviscosity factor of 0.067.[42] The oblate slip microviscosity factor would effectively increase the MEI^+ *a* values obtained from eq 7 from 1.12 and 1.17 Å to 2.45 and 2.56 Å, whereas the prolate slip microviscosity factor would effectively increase the MEI^+ hydrodynamic radii values obtained from eq 7 from 1.12 and 1.17 Å to 2.76 and 2.88 Å. These "corrected" *a* values are reasonably close to the value of 3.2 Å assumed for the molecular radius of MEI^+ (Figure 1).

Summary. The ^{13}C and ^{27}Al NMR and ^1H DOSY results for a 1:1 $EtAlCl_2$−MEICl melt provide a direct correlation between ^{13}C and ^{27}Al rotational correlation times, self-diffusion coefficients, and viscosity. These relationships support the concept that the transport properties of this melt are determined by the molar quantities of the salt and not by individual properties of the ions in the melt.[43] Use of the Stokes−Einstein−Debye model of the 1:1 $EtAlCl_2$−MEICl melt produces unreasonable values for the Stokes radius of MEI^+ which can be corrected by the use of appropriate microviscosity factors.[41,42] The comparisons of viscosities, MEI^+ ^{13}C rotational correlation times, ^1H diffusion coefficients, and $EtAlCl_2$ ^{27}Al rotational correlation times support the existence of MEI^+−$EtAlCl_2$ interactions in a 1:1 $EtAlCl_2$−MEICl melt.

Acknowledgment. This work was partially funded by NSF Grant CHE-9524865 (W.R.C.) and CHE-9524514 (C.K.L.). We would also like to thank Dr. Charles S. Johnson, Jr., for the computer programs used in processing the DOSY data.

References and Notes

(1) Carper, W. R.; Pflug, J. L.; Elias, A. M.; Wilkes, J. S. *J. Phys. Chem.* **1992**, *96*, 3828−3833.
(2) Keller, C. E.; Carper, W. R. *J. Phys. Chem.* **1994**, *98*, 6865−6869.
(3) Larive, C. K.; Lin, M.; Piersma, B. J.; Carper, W. R. *J. Phys. Chem.* **1995**, *99*, 12409−12412.
(4) Carper, W. R.; Mains, G. J.; Piersma, B. J.; Mansfield, S. L.; Larive, C. K. *J. Phys. Chem.* **1996**, *100*, 4724−4728.
(5) Gilbert, B.; Chauvin, Y.; Guibard, I. *Vibr. Spectrosc.* **1991,** *1*, 299.
(6) Keller, C. E.; Carper, W. R.; Piersma, B. J. *Inorg. Chim. Acta* **1993,** *209*, 239.
(7) Keller, C. E.; Carper, W. R. *Inorg. Chim. Acta* **1993,** *210*, 203.
(8) Weidlein, J. *J. Organomet. Chem.* **1969**, *17*, 213−222.
(9) Yamamoto, O.; Hayamizu, K.; Yanigisawa, M. *J. Organomet. Chem.* **1974**, *73*, 17−25.
(10) Benn, R.; Rufinska, A. *Angew. Chem., Int. Ed. Engl.* **1986**, *25*, 861−881.
(11) Benn, R.; Rufinska, A.; Lehmkuhl, H.; Janssen, E.; Kruger, C. *Angew. Chem., Int. Ed. Engl.* **1983**, *22*, 779−780.
(12) Morris, K. F.; Johnson, C. S., Jr. *J. Am. Chem. Soc*. **1992**, *114*, 3139−3141.
(13) Boere, R. T.; Kidd, R. G. In *Annual Reports on NMR Spectroscopy*; Webb, G. A., Ed.; Academic Press: New York, 1982; Vol. 13, pp 319−385.
(14) Wilkes, J. S.; Levisky, J. A.; Wilson, R. A.; Hussey, C. L. *Inorg. Chem.* **1982**, *21*, 1263−1264.
(15) Neuhaus, D.; Williamson, M. *The Nuclear Overhauser Effect in Structural and Conformational Analysis*; VCH Publishers: New York, 1989; p 56.
(16) Gibbs, S. J.; Johnson, C. S., Jr. *J. Magn. Reson*. **1991**, *93*, 395−402.
(17) Lin, M.; Jayawickrama, D. A.; Rose, R. A.; DelViscio, J. A.; Larive, C. K. *Anal. Chim. Acta* **1995**, *307*, 449−457.
(18) Morris, K. F.; Johnson, C. S., Jr. *J. Am. Chem. Soc*. **1993**, *115*, 4291−4299.
(19) Morris, K. F.; Stilbs, P.; Johnson, C. S., Jr. *Anal. Chem*. **1994**, *66*, 211−215.
(20) Provencher, S. W.; Vogel, R. H. In *Numerical Treatment of Inverse Problems in Differential and Integral Equations*; Dueflhard, P., Hairer, E., Eds.; Birkhauser: Boston, 1983; pp 304−319.
(21) Vogel, R. H. *SPLMOD Users Manual Technical Report DA06*; European Molecular Biology Laboratory, Heidelberg, 1983.
(22) (a) Abragam, A. *Principles of Nuclear Magnetism*; Oxford University Press: Oxford, U.K., 1961; Chapter 8. (b) McConnell, J. *The Theory*

of Nuclear Magnetic Relaxation in Liquids; Cambridge University Press: Cambridge, U.K., 1987.

(23) Kuhlmann, K. F.; Grant, D. M. *J. Am. Chem. Soc.* **1978**, *90*, 7355−7357.

(24) (a) Farrar, T. C.; Becker, E. D. *Pulse and Fourier Transform NMR*; Academic Press: New York, 1971. (b) Spiess, H. W. *NMR* **1978**, *15*, 55−214. (c) Canet, D.; Robert, J. B. *NMR* **1990**, *25*, 46−89. (d) Halle, B.; Wennerstrom, H. *J. Magn. Reson.* **1981**, *44*, 89−100

(25) Mitchell, R. W.; Eisner, J. *J. Chem. Phys.* **1960**, *33*, 86−91.

(26) Mitchell, R. W.; Eisner, J. *J. Chem. Phys*. **1961**, *34*, 651−654.

(27) Waylishen, R. E.; Pettitt, B. A.; Danchura, W. *Can. J. Chem*. **1977**, *55*, 3602−3608.

(28) Kivelson, D.; Kivelson, M. G.; Oppenheim, I. *J. Chem. Phys.* **1970**, *52*, 1810−1821.

(29) Tyrrell, H. J. V.; Harris, K. R. *Diffusion in Liquids*; Butterworth: London, U.K., 1984.

(30) McLaughlin, E. *Trans. Faraday Soc*. **1959**, *55*, 28−38.

(31) Keller, C. E.; Carper, W. R. *J. Magn. Reson*., *Ser. A* **1994**, *A110*, 125−129.

(32) Keller, C. E.; Carper, W. R. *Inorg. Chim. Acta* **1995**, *238*, 115−120.

(33) Keller, C. E.; Piersma, B. J.; Mains, G. J.; Carper, W. R. *Inorg. Chem.* **1994**, *33*, 5601−5603.

(34) Dewar, M. J. S.; Patterson, D. B.; Simpson, W. I. *J. Am. Chem. Soc.* **1971**, *93*, 1030−1032.

(35) Fannin, A. A.; Floreani, D. A.; King, L. A.; Landers, L. S.; Piersma, B. J.; Stech, D. J.; Vaughn, R. L.; Wilkes, J. S.; Williams, J. L. *J. Phys. Chem*. **1984**, *88*, 2614−2621.

(36) Carper, W. R.; Pflug, J. L.; Wilkes, J. S. *Inorg. Chim. Acta* **1992**, *193*, 201−205.

(37) Dieter, K. M.; Dymek, C. J.; Heimer, N. E.; Rovang, J. W.; Wilkes, J. S. *J. Am. Chem. Soc.* **1988**, *110*, 2722−2726.

(38) Dymek, C. J.; Stewart, J. J. P. *Inorg. Chem.* **1989**, *28*, 1472−1476.

(39) Dymek, C. J., Jr.; Grossie, D. A.; Fratini, A. V.; Adams, W. W. *J. Mol. Struct*. **1989**, *213*, 25−34.

(40) Stewart, J. J. P. *J. Comput. Chem.* **1989**, *10*, 209−220.

(41) Gierer, A.; Wirtz, K. *Z. Naturforsch*. **1953**, *8A*, 522−532.

(42) Hu, C. M.; Zwanzig, R. *J. Chem. Phys.* **1974**, *60*, 4354−4357.

(43) Weiden, N.; Wittekopf, B.; Weil, K. G. *Ber. Bunsen-Ges. Phys. Chem*. **1990**, *94*, 353−358.